

# Lattice expansion and evolution of damage buildup in Be-implanted InAs

Q.W. Wang<sup>a</sup>, C.H. Sun<sup>a</sup>, M. Chen<sup>b</sup>, S.H. Hu<sup>a</sup>, J. Wu<sup>a</sup>, Y. Sun<sup>a</sup>, G.J. Hu<sup>a</sup>, X. Chen<sup>a</sup>, H.Y. Deng<sup>a,\*</sup>, N. Dai<sup>a,\*</sup>

<sup>a</sup> National Laboratory for Infrared Physics, Shanghai Institute of Technical Physics, Chinese Academy of Sciences, Shanghai 200083, People's Republic of China

<sup>b</sup> School of Physics, Shandong University, Jinan 250100, People's Republic of China

## ARTICLE INFO

### Article history:

Received 3 June 2011

Received in revised form 22 July 2011

Available online 30 July 2011

### Keywords:

III–V Semiconductors

Ion-implantation

HRXRD

Microstructure

Indium arsenide

## ABSTRACT

The lattice expansion in InAs single crystal, due to ion-implantation by 80 keV Be ions with the implantation fluencies ranging from  $1 \times 10^{12}$  to  $2 \times 10^{16} \text{ cm}^{-2}$ , has been investigated by using high resolution X-ray diffraction (HRXRD), transmission electron microscopy (TEM), and Rutherford backscattering spectrometry/channeling (RBS/C). In order to clarify the evolution of damage buildup, the nonlinear maximum perpendicular strain  $\varepsilon_m$  as a function of the Be fluence was obtained and analyzed. The curve of  $\varepsilon_m$  vs. Be fluence is subdivided into five regions, each having a different damage accumulation behavior. The involved probable mechanisms of microstructural variation in InAs due to Be implantation of different fluencies are analyzed in detail.

© 2011 Elsevier B.V. All rights reserved.

## 1. Introduction

The compound semiconductor InAs with narrow band gap and high electron mobility is a popular material for applications in high-speed and infrared optoelectronics devices [1–3]. Ion implantation has been widely used for intentional impurity doping in semiconductor device technologies. Unfortunately, as a non-equilibrium processing, ion implantation often causes damage, strain, and crystalline-to-amorphous phase transformation in virgin substrates. Although most of the damages can be removed by rapid thermal annealing, some kinds of lattice damages are irreversible especially when the amorphous phase occurs. Owing to their light atom mass, two valence electrons and low damage introduction rate, Be ions are an optimum choice of *p*-type doping for InAs through ion implantation. The microscopic structural variation in crystalline InAs caused by ion-implantation, however, is not well understood, due to its binary complexity and associated lattice defects compared to elemental semiconductors such as Si and Ge. Pearson et al. had investigated the damage and recrystallization in Si- and Mg-implanted InAs prior to and after annealing [4]. The annealing properties of InAs implanted by 400 keV Fe or Ti had been reported [5]. Gerasimenko et al. had investigated the Be distribution in Be-implanted InAs before and after annealing [6]. Recently, Gonzalez-Arrabal et al. had a research on the depth dependent lattice disorder and strain in Mn-implanted InAs film grown by atomic layer molecular beam epitaxy prior to and after

rapid thermal annealing processes [7]. Systematical studies focusing on the ion-implantation-induced lattice expansion and evolution of damage buildup have been investigated on Si, Ge, GaAs, InP, and GaN [8–20]. Similar work has not been done on InAs. Implantation-induced damages and crystal distortion strongly affect device performance. It is thus essential to systematically investigate lattice expansion in order to clarify microscopic structural variation and evolution of the damage buildup in Be-implanted InAs at different implantation fluencies.

In this paper, InAs samples were implanted with Be. The implantation energy was 80 keV and the fluence was varied from  $1.0 \times 10^{12}$  to  $2.0 \times 10^{16} \text{ cm}^{-2}$ . High resolution X-ray diffraction (HRXRD) was performed along (1 0 0) direction on Be-implanted InAs in  $2\theta$ - $\omega$  scan mode to monitor the change of (4 0 0) diffraction peak. New peaks were observed near the InAs (4 0 0) line. The peaks initially grew up and shifted towards low angle with increasing fluence. However, all the peaks shrunk and almost disappeared finally with larger implantation fluence. The new peaks were attributed to the Be-implantation-induced lattice expansion. The maximum perpendicular strain  $\varepsilon_m$  induced by lattice expansion as a function of the Be fluence was obtained. This curve could be subdivided into five regions representing different mechanisms of microscopic structural variation and evolution of the damage buildup. As the complementary techniques, Rutherford backscattering spectrometry/channeling (RBS/C) and transmission electron microscopy (TEM) were also performed to investigate the evolution of the damage buildup inside the implanted layer.

## 2. Experimental

The InAs used for implantation was *n*-type ( $n \sim 10^{16} \text{ cm}^{-3}$  at room temperature) one side well-polished undoped EPI-ready

\* Corresponding authors. Tel.: +86 021 25051418; fax: +86 021 65830734 (H.Y. Deng), tel.: +86 021 25051003; fax: +86 021 65830734 (N. Dai).

E-mail addresses: [hydeng@mail.sitp.ac.cn](mailto:hydeng@mail.sitp.ac.cn) (H.Y. Deng), [ndai@mail.sitp.ac.cn](mailto:ndai@mail.sitp.ac.cn) (N. Dai).

single crystal wafer with (1 0 0) direction and  $450 \pm 25 \mu\text{m}$  thickness, which was grown by liquid encapsulated Czochralski (LEC) method. Before implantation the substrates were cleaned by organic solvent in a supersonic cleaner. Implantation of 80 keV Be ions was performed at room temperature with the fluence ranging from  $1 \times 10^{12}$  to  $2 \times 10^{16} \text{ cm}^{-2}$ . To avoid the beam-induced heating effect, the current density was about  $250 \text{ nA/cm}^2$ . The Be-ion beam incidence is at  $7^\circ$  off the (1 0 0) direction, in order to minimize the channeling effect. The computer simulation results of the distribution of Be ions and implantation-created vacancies were calculated by SRIM2008 [21]. Both the Be-distribution and vacancy-distribution show a Gaussian-like shape with the center located at  $\sim 0.31$  and  $\sim 0.23 \mu\text{m}$  respectively. Using the Bruker D8 Discover diffractometer, the HRXRD spectra were measured by the  $\text{Cu } K_{\alpha 1}$  line with the wavelength of  $0.15406 \text{ nm}$ . The secondary ion mass spectroscopy (SIMS) measurement on selected samples was performed by CAMECA IMS-6F. The cross-section TEM images were measured on the specimens prepared by Ar ion milling with liquid nitrogen cooling to keep damage stable. The TEM measurement was operated at  $200 \text{ kV}$ . RBS/C was performed along the (1 0 0) direction using  $2.1 \text{ MeV } ^4\text{He}^+$  ions and with the detector positioned at about  $165^\circ$  with respect to the ion beam direction.

### 3. Result and discussion

The HRXRD spectra near the (4 0 0) diffraction peak of the InAs samples at different fluencies are shown in Fig. 1. To simply clarify the change of peaks appeared after implantation, the curves are normalized by the (4 0 0) diffraction peak of the InAs substrate. When the fluence below  $2 \times 10^{13} \text{ cm}^{-2}$ , the (4 0 0) peaks of implanted samples are almost same as that of virgin InAs. At the fluence of  $2 \times 10^{13} \text{ cm}^{-2}$ , a new peak shows up on the low-angle side of the InAs (4 0 0) diffraction line and, with increasing fluence, the peak grows up and shifts further to lower-angle side. In the meanwhile the peak intensity also increases and reaches to its maximum value at the fluence of  $2 \times 10^{15} \text{ cm}^{-2}$ . From  $2 \times 10^{15}$  to  $8 \times 10^{15} \text{ cm}^{-2}$  fluence range, the intensity of the new peak remains almost unchanged, while the peak keeps shifting to the lower angle. At the fluence of  $4 \times 10^{15} \text{ cm}^{-2}$ , a second peak shows up. As shown in Fig. 1, from  $8 \times 10^{15}$  to  $1.2 \times 10^{16} \text{ cm}^{-2}$ , the first peak begins to shrink and the second one grows up and reaches the maximum at the fluence of  $1.2 \times 10^{16} \text{ cm}^{-2}$ . A third peak appears at the fluence of  $1.0 \times 10^{16} \text{ cm}^{-2}$ . For the fluence range from  $1.2 \times 10^{16}$  to  $2.0 \times 10^{16} \text{ cm}^{-2}$ , all the new peaks shrink dramatically. The new peaks merge into a weak wide peak at the fluence of above  $1.6 \times 10^{16} \text{ cm}^{-2}$ .

In order to investigate the change of implantation induced microstructures, the HRXRD measurements also performed on the selected samples to monitor the Be-implanted InAs (2 0 0) line. As shown in Fig. 2(a), new peaks near (2 0 0) and (4 0 0) lines appear in pairs after Be implantation with  $2 \times 10^{15} \text{ cm}^{-2}$  fluence. A  $2\theta$ - $\omega$  scan measurement from  $10^\circ$  to  $90^\circ$  was also performed, which shows no additional peaks in the range scanned. A high resolution TEM image of the implanted area is presented in Fig. 2(b). Obviously, the implanted area keeps the same zinc blende structure as that of the InAs substrate, although some damage is expected. This is also confirmed by the presented fast Fourier transformation pattern in Fig. 2(c). Hence, the possibility of formation of a new phase after the implantation is excluded. And so the new HRXRD peaks at lower-angle side of the (4 0 0) diffraction line of the InAs substrate are due to the Be-implanted layer that has a larger lattice constant than that of the InAs substrate. It means that the InAs lattice in the Be-implanted layer is expanded. Raising the fluence leads to increasing lattice expansion, companied by the enhancement of the first new peak in the HRXRD curve and its shift

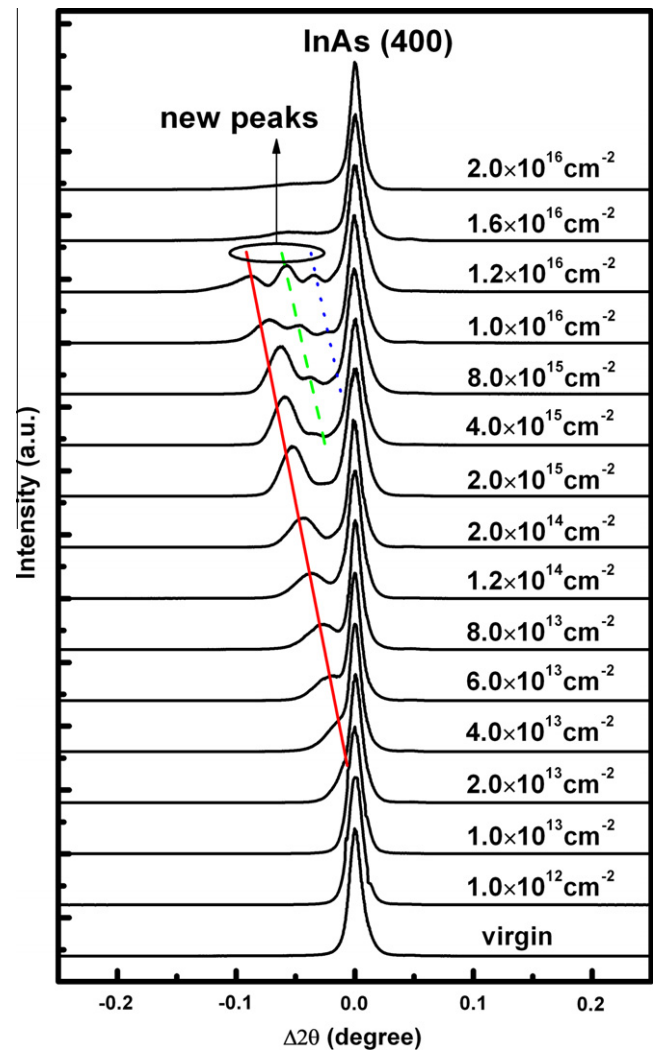


Fig. 1. Normalized (4 0 0) HRXRD spectra of InAs implanted by 80 keV Be ions with different fluencies at room temperature, in which the red, green dash and blue dot lines point out the evolution of positions of the first, second, and third new peaks, respectively. (For interpretation of the references to color in this figure legend, the reader is referred to the web version of this article.)

to lower angle, as shown in Fig. 1. The second and the third new peaks, occurring at the fluence larger than  $2 \times 10^{15} \text{ cm}^{-2}$ , are originated from the nonuniform lattice expansion in the implanted layer. It can be interpreted with the aid of a kinematical model for X-ray diffraction in nonuniform crystalline films [14], which indicates the expanded lattice has a distribution with depth in the implanted layer. Due to the accumulated damages, the implanted layer becomes highly disordered and the amorphous component might arise with increasing fluence (above  $1.6 \times 10^{16} \text{ cm}^{-2}$ ), so that the sharp XRD peaks could not be observed. The highly disordered region may also be originated from strain relaxation to certain extent, which is the reason why a wide and low intensity peak is observed at high fluence.

To gain insight into the lattice expansion in detail, a computer simulation by SRIM 2008 [21] is performed and the distribution of Be ions and implantation-created vacancies in InAs are shown in Fig. 3(a). In the simulation, the density of InAs was chosen to be  $5.667 \text{ g/cm}^3$  [23], the ratio of III and V components in InAs was taken as 1:1, and the angle of the incident beam was  $7^\circ$  off the normal of the surface. Vacancies distributions were calculated at the displacement energies of  $6.7 \text{ eV}$  for In and  $8.3 \text{ eV}$  for As [22]. The profile of total vacancies is slightly shifted with respect to that

Download English Version:

<https://daneshyari.com/en/article/1685522>

Download Persian Version:

<https://daneshyari.com/article/1685522>

[Daneshyari.com](https://daneshyari.com)